ISSN 2394-3777 (Print)
ISSN 2394-3785 (Online)
Available online at www.ijartet.com
International Journal of Advanced Research Trends in Engineering and Technology (IJARTET)
Vol. 4, Special Issue 12, March 2017

DYNAMIC REGION BASED INTEGRATION TECHNIQUE FOR SKIN CANCER DETECTION

Ms.Sneha.S[1], Mr.M.K.Jayakumar[2]

Assistant Professor, Mechatronics Engineering, Sri Krishna College of Engineering and Technology, Coimbatore, India [1]

Assistant Professor, Aeronautical Engineering, Nehru Institute of Engineering and Technology, Coimbatore, India [2]

Abstract: Melanoma is the deadliest form of skin cancer diseases. Affecting rates of melanoma have been developed, particularly among non- Hispanic white humans, however survival rates are high if detected early period. Because of the costs for dermatologists to screen every patient affected by this diseases. So need for an automated system to assess a patient's risk of melanoma using images of their skin lesions captured using a standard digital camera lenses. The difficult in implementing such a system is locating the skin lesion in the digital image way. Skin lesion of a novel texture-based segmentation algorithm is developed here. The proposed segmentation framework is tested by comparing lesion segmentation results and melanoma classification results to results using other state-of-art algorithms. Here the framework has higher segmentation accuracy compared to all other tested algorithms.

Keywords: Melanoma, texture, algorithm, segmentation, framework.

I. INTRODUCTION

Melanoma is a cancer of the melanocytes, the cell found in the skin's epidermis that produces melanin. Melanoma most commonly occurs on the trunk or lower extremities. While malignant melanoma is less common than non-melanoma skin cancer, it is considered the most deadly form of skin cancer. This is because melanoma accounts for approximately 75% of deaths associated with skin cancer. In 2013, it is estimated that 76,680 people will be diagnosed with melanoma and 9,480 people will die of melanoma in the United States. In Canada, 1 in 74 men and 1 in 90 women will develop melanoma in their lifetime. The recent trends in melanoma incidence rates are more alarming.

A study of the melanoma trends from 1992-2006 found that incidence rates for non-Hispanic white males and females were increasing at an annual rate of approximately 3%. For young adults ages 15-30, melanoma is one of the most commonly diagnosed forms of cancer. If melanoma is detected early, while it is classified at stage I (less than 0.76 mm thick), the 5-year survival rate is 96%. However, the 5-year survival rate decreases to 5% if the melanoma is in stage IV. The cost of treatment of stage IV melanoma is also 30 times the cost of treatment for stage I melanoma. With the rising incidence rates in certain subsets of the general population, early melanoma screening is beneficial. Early automated melanoma screening systems assess the risk of melanoma using images acquired via a digital dermatoscope. A dermatoscope is a special device for dermatologists to use to look at skin lesions that acts as a filter. Pictures acquired through a digital dermatoscope are referred to as dermoscopy images and have relatively low levels of noise and consistent background interference. Pre-processing algorithms applied to dermatological images include normalizing or enhancing image colors.

However, requiring dermatologists to have a dermatoscope impedes the adoption of these systems as only 48% of practicing dermatologists use dermatoscopes. The most common reasons against using the dermatoscope include a lack of teaching.

Nowadays work with automated melanoma screening algorithms tries to adapt the algorithms to analyse images taken by a standard digital camera. There is a need for a segmentation algorithm designed specifically for digital images of skin lesions. Before extracting features from the skin lesion and classifying the lesion as malignant or benign, the location of the lesion border must be identified using segmentation problems. Obtaining an accurate estimate of the lesion border is important because of the types of features used for classification. One common set of features

ISSN 2394-3777 (Print)
ISSN 2394-3785 (Online)
Available online at www.ijartet.com
International Journal of Advanced Research Trends in Engineering and Technology (IJARTET)
Vol. 4, Special Issue 12, March 2017

is the ABCD scale: symmetry, corner irregularity, the color variegation. In particular, metrics that measure border irregularity may depend heavily on the accuracy of the estimated lesion corner. So it is important that the skin lesion segmentation algorithm is correct, as output segmentation is used as an input to feature extraction and melanoma classification algorithms method. Few segmentation algorithms have been proposed to locate skin lesion in images simultaneously. Many of proposed segmentation algorithms are only applicable to dermoscopy images, which has better contrast between the lesion and surrounding skin area for certain types of lesions.

II. PROPOSED ALGORITHM

Another challenge is in the segmentation step, which is the step where the border of the lesion is identified. While images acquired using the dermatoscope have been magnified and enhanced to better identify the lesion, standard digital images taken by a digital camera do not have those advantages. Illumination variation, textural patterns of skin, and noise can make separating normal skin and lesion difficult in digital images. Based on these two challenges, there is a need for a robust segmentation algorithm that is designed specifically for images of lesions taken with a standard digital camera. This algorithm should incorporate correcting for illumination variation as a pre-processing step. This thesis proposes a novel skin lesion segmentation algorithm to solve these two challenges.

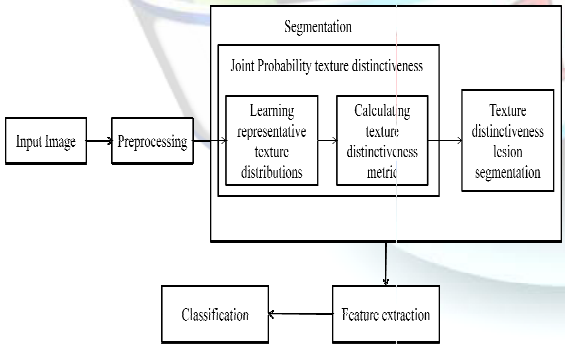

Fig.1. Algorithm flow chart highlighting steps in the JPTD algorithm

We obtain an initial rain map from an image frame, which is then refined based on sparse representation and classification. Finally, were constructing a rain-free frame by exploiting the information in adjacent frames Fig.1shows an overview of the proposed algorithm. First, we obtain an initial rain map by computing the difference between a current frame and an optimally warped frame. Second, we decompose the initial rain map using sparse basis vectors, and employ an SVM classifier to dichotomize those vectors into valid ones and outliers. We then reconstruct are fine d rain map by employing the valid vectors only. Finally, were place rainy pixels with rain-free values, by formulating the rain streak removal as a matrix completion problem?

A. *Sparse texture model*

Sparse texture models find a small number of texture identification, like texture patches, to find the property an entire picture. The sparse texture models learn important local texture details present in a picture. By the use of a sparse texture model allows the image to be stored efficiently and allows for efficient computation of algorithms that involve textures from the picture. So many ways to learn the model, including clustering or by formulating the problem as an optimization problem. A common method to learn a sparse texture model is by employing a dictionary learning algorithm, where a set of texture patches that can best match details in the original image is learned.

B. *Dynamic Region Merging (DRM)*

Automatic image segmentation can be phrased as an inference problem [1]. For example, we might observe the colors in an image, which are caused by some unknown principles. In the context of image segmentation, the observation of an image is given but the partition is unknown. In this respect, it is possible to formulate the inference problem as finding some representation of the pixels of an image, such as the label that each pixel is assigned. With this label, an image is partitioned into a meaningful collection of regions and objects.

The Gestalt laws in psychology [26-27] have established some fundamental principles for this inference problem. For example, they imply some well-defined perceptual formulations for image segmentation, such as homogeneous, continuity and similarity. In the family of region merging techniques, some methods have used statistical similarity tests [16] [29] to decide the merging of regions, where a predicate is defined for making local decisions. These are good examples of considering the homogeneity characteristics within a region, from which we can see that an essential attribute for region merging is the consistency of data elements in the same region. In other words, if neighbouring regions share a common consistency property, they should belong to the same

ISSN 2394-3777 (Print)
ISSN 2394-3785 (Online)
Available online at www.ijartet.com
International Journal of Advanced Research Trends in Engineering and Technology (IJARTET)
Vol. 4, Special Issue 12, March 2017

group. However, most of the existing region merging algorithms cannot guarantee a globally optimal solution of the merging result; in other words, the region merging output is either over-segmented or under-segmented. In this section, we propose a novel predicate which leads to certain global properties for the segmentation result. 5 The proposed predicate is based on measuring the dissimilarity between pixels along the boundary of two regions. For the convenience of illustrating the whole framework, we use the definition of region adjacency graph (RAG) [30] to represent an image. Let G = (V, E) be an undirected graph, where vi∈V is a set of nodes. [5] proposed a principle in which another NN yield input control law was created for an under incited quad rotor UAV which uses the regular limitations of the under incited framework to create virtual control contributions to ensure the UAV tracks a craved direction. Utilizing the versatile back venturing method, every one of the six DOF are effectively followed utilizing just four control inputs while within the sight of un demonstrated flow and limited unsettling influences. Elements and speed vectors were thought to be inaccessible, along these lines a NN eyewitness was intended to recoup the limitless states. At that point, a novel NN virtual control structure which permitted the craved translational speeds to be controlled utilizing the pitch and the move of the UAV. At long last, a NN was used in the figuring of the real control inputs for the UAV dynamic framework. Utilizing Lyapunov systems, it was demonstrated that the estimation blunders of each NN, the spectator, Virtual controller, and the position, introduction, and speed following mistakes were all SGUUB while unwinding the partition Principle.

III. SYSTEM IMPLEMENTATION

A. *Illumination adjustment*

Background correction can be applied while acquiring images (a priori) or after acquisition (a posteriori). The difference between these is that a priori correction uses additional images obtained at the time of image capture while in a posteriori correction, the additional images are not available and therefore an ideal illumination model has to assume. The a priori methods are therefore the preferred option.

When digitising images there are several sources of image degradation to consider:

1. Camera noise
   - Random noise. This is due to uncorrelated fluctuations above and below the image data as a consequence to the nature of the image sensors.
   - Fixed pattern noise (“hot pixels”) is characterised by pixel intensities that are consistently above random noise fluctuations and it is due to faulty CCD or pixel differences in charge leakage rate (this is also called “electronic bias” of the sensor).
   - Banding noise may arise during the process of reading the data from the digital sensor or by interference with other electronic equipment. This type of periodic noise can be corrected to some extent with Fourier filtering.

2. The colour temperature of the light source also affects image quality. Light sources have a characteristic radiation spectrum. In most filament light bulbs this spectrum varies depending the temperature of the filament (i.e. the voltage applied to the lamp; with lower voltage the light becomes yellow- reddish while with higher voltage, it becomes bluish). Therefore, images taken at different times may exhibit backgrounds with slightly different hues. This makes it difficult to standardise procedures such as colour segmentation, colour separation, hue quantification, etc. Some microscopes have a switch to set a preset voltage to the bulb so it delivers a particular intensity and colour temperature (typically about 3200K to match indoor type B photographic film). When fixed voltages are used, then the intensity of the light is typically controlled with neutral density filters in the light path.

B. *Color Space*

In the implementation of the TDLS algorithm, the picture is in the RGB domain and has three channels (a = 3). However, the algorithm can be generalized and expanded to take into account multi- or hyper spectral images of a skin lesion. For standard digital images, we convert the image to the XYZ color space to find texture distributions and during the initial over segmentation.

C. *Image Segmentation*

In computer vision, image segmentation is the process of partitioning a digital image into multiple segments. The goal of segmentation is to simplify and/or change the representation of an image into something that is more meaningful and easier to analyse. Image segmentation is typically used to locate objects and boundaries in images. More precisely, image segmentation is the process of assigning a label to every pixel in an image such that pixels with the same label share certain characteristics.

The result of image segmentation is a set of segments that collectively cover the entire image, or a set of contours extracted from the image (see edge detection). Each of the pixels in a region is similar with respect to some

ISSN 2394-3777 (Print)
ISSN 2394-3785 (Online)
Available online at www.ijartet.com
International Journal of Advanced Research Trends in Engineering and Technology (IJARTET)
Vol. 4, Special Issue 12, March 2017

characteristic or computed property, such as color, intensity, or texture. Adjacent regions are significantly different with respect to the same characteristic(s) [1]. When applied to a stack of images, typical in medical imaging, the resulting contours after image segmentation can be used to create 3D reconstructions with the help of interpolation algorithms like marching cubes.

D. Algorithm Steps

Input: the initially over segmented image S0. Output: region merging result.

1. Set i=0.
2. For each region in segmentation Si, use Algorithm 1 to check the value of predicate P with respect to its neighbouring regions.
3. Merge the pairs of neighbouring regions whose predicate P is true, such that segmentation Si+1 is constructed.
4. Go back to step 2 until Si+1 = Si.
5. Return Si machines. The Haar wavelet's mother wavelet function $\psi(t)$ can be described as

$$\psi(t) = \begin{cases} 1 & 0 \le t < \frac{1}{2}, \\ -1 & \frac{1}{2} \le t < 1, \\ 0 & \text{otherwise.} \end{cases}$$

IV. PROPERTIES OF THE PROPOSED DRM ALGORITHM

Although the proposed DRM scheme is conducted in a greedy style, some global properties of the segmentation can be obtained. More specifically, it can be proved that the proposed DRM algorithm produces a segmentation S which is neither over- merged nor under-merged according to the proposed predicate P. Similar to the definitions of over-segmentation and under-segmentation in [18], we define the concepts of over-merged segmentation and under-merged segmentation as below Definition1 under-merged segmentation. A segmentation S is under-merged if it contains some pair of regions for each there is an evidence of a merging between the regions Definition2 Over-merged segmentation. A segmentation S is over-merged, if there is another segmentation Sr which is not under-merged and each region of Sr is contained in some component of S. Or saying, Sr can be obtained by splitting one or more regions of S. We call that Sr is a refinement of S. Definition3 the evidence of boundary. There is an evidence of boundary between a pair of regions R1 and R2 if the predicate P is false because the inconsistency property between them does not hold, Lemma 1. If two adjacent regions are not merged for an evidence of a boundary between them in the k^{th} iteration, they will be in different regions in the final segmentation. Denote by Ri k and Rj k two neighboring regions in the k^{th} iteration. Then Ri = Ri k and Rj = Rj k , where Ri is the region whose label is Li and Rj is the region whose label is Lj in the final segmentation S. Proof: If there is an evidence of a boundary between Ri k and Rj k , according to Definition 3.

- Lemma 1 holds because our merging predicate relies on comparing the minimum weight edge between regions. We can prove that with this measure, some global properties of the segmentation can be easily obtained, Theorem1. The segmentation S by Algorithm 2 is not under-merged according to Definition 1. Proof: If S is under-merged, there must be some pair of regions Ri k and Rj k that do not cause a merge in the merging process. Therefore, the evidence of a boundary does not hold for Ri k and Rj k. According to Lemma 14 1, if Ri k and Rj k are not merged, Ri = Ri k and Rj = Rj k. This implies that Algorithm 2 does not merge Ri k and Rj k. The evidence of a boundary holds for them, which is a contradiction.
- Theorem 2: The segmentation S by Algorithm 2 is not over-merged according to Definition 2. Proof: If S is over-merged, there must be a proper refinement T that is not under-merged. Let a region $C \subset S$, and there are two adjacent regions $A \subset C$, $B \subset C$, such that A and B satisfy the refinement T. According to Algorithm 2, A and B will not merge with any other regions in C before they merge with each other. Then C does not contain A and B, which is a contradiction.

V. SIMULATION RESULTS

The TD maps are compared visually. Select skin lesion images from the Dermquest database are used for different, the corrected for illumination variation using the MSIM algorithm. These examples are selected because they highlight cases with significant differences between the TD and TDLS algorithms and are shown in Fig. 3. Also, the dynamic range of pixels is scaled to the maximum pixel intensity and also the minimum pixel

ISSN 2394-3777 (Print)
ISSN 2394-3785 (Online)
Available online at www.ijartet.com
International Journal of Advanced Research Trends in Engineering and Technology (IJARTET)
Vol. 4, Special Issue 12, March 2017

intensity, resulting in a different dynamic range for each TD map.

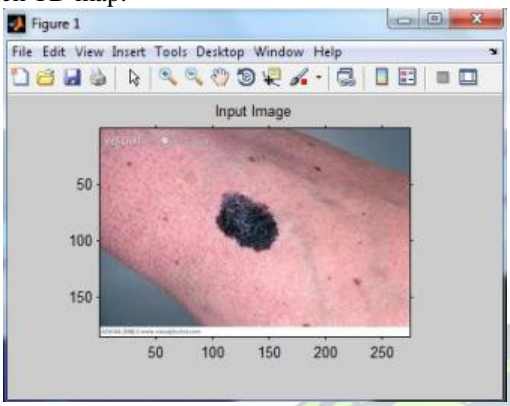

Fig.2. Input Image

Fig.3. Illumination Adjusted Image

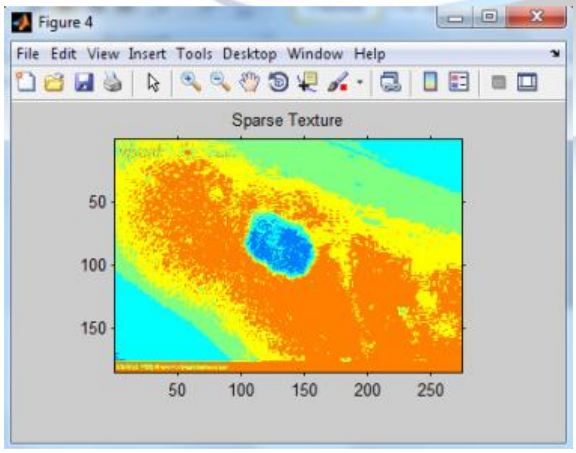

Fig.4. Sparse Texture of Input Image

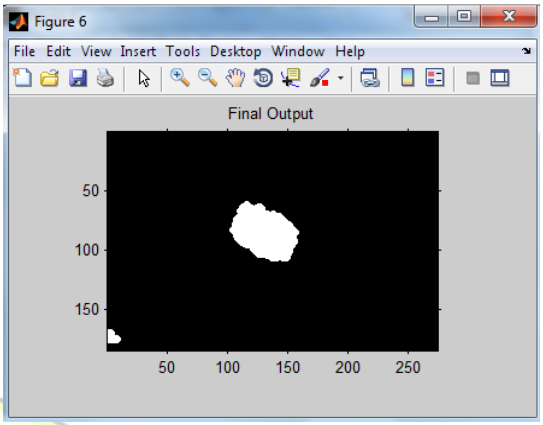

Fig.5. Segmentation Output

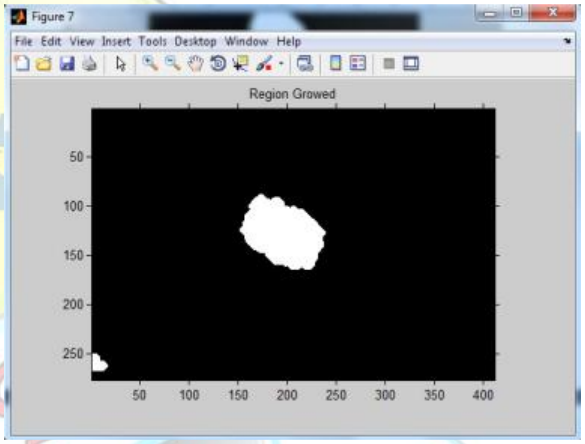

Fig.6. Region Growing Technique Output

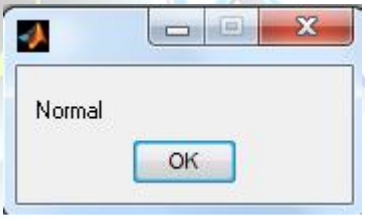

Fig.7. Classification Result

REFERENCES

[1] S. G. Narasimhan and S. K. Nayar, "Vision and the atmosphere," Int.J. Comput. Vis., vol. 48, no. 3, pp. 233–254, Jul. 2002.

[2] K. Garg and S. K. Nayar, "Vision and rain," Int. J. Comput. Vis., vol. 75, no. 1, pp. 3–27, Oct. 2007.

[3] L.-W. Kang, C.-W.Lin, and Y.-H. Fu, "Automatic single-image-based rain streaks removal via image decomposition," IEEE Trans. Image Process., vol. 21, no. 4, pp. 1742–1755, Apr. 2012.

[4] H. Hase, K. Miyake, and M. Yoneda, "Real-time snowfall noise elimi- nation," in Proc. IEEE ICIP, Oct. 1999, pp. 406–409.

[5] Christo Ananth,"A NOVEL NN OUTPUT FEEDBACK CONTROL LAW FOR QUAD ROTOR UAV",International Journal of Advanced Research in Innovative Discoveries in Engineering and Applications[IJARIDEA],Volume 2,Issue 1,February 2017,pp:18-26.

[6] K. Garg and S. K. Nayar, "When does a camera see rain?" in Proc. 10th IEEE ICCV, Oct. 2005, pp. 1067–1074.

[7] X. Zhang, H. Li, Y. Qi, W. K. Leow, and T. K. Ng, "Rain removal in video by combining temporal and chromatic properties," in Proc. IEEE ICME, Jul. 2006, pp. 461–464.

[8] P. C. Barnum, S. Narasimhan, and T. Kanade, "Analysis of rain and snow in frequency space," Int. J. Comput. Vis., vol. 86, nos. 2–3, pp. 256–274, Jan. 2010.

[9] M. Shen and P. Xue, "A fast algorithm for rain detection and removal from videos," in Proc. IEEE ICME, Jul. 2011, pp. 1–6.

[10] V. Santhaseelan and V. K. Asari, "A phase space approach for detection and removal of rain in video," Proc. SPIE, vol. 8301, p. 830114, Jan. 2012.

[11] L.-W. Kang, C.-W.Lin, C.-T.Lin, and Y.-C. Lin, "Self-learning-based rain streak removal for image/video," in Proc. IEEE ISCAS, May 2012, pp. 1871–1874.

[12] J. Chen and L.-P.Chau, "A rain pixel recovery algorithm for videos with highly dynamic scenes," IEEE Trans. Image Process., vol. 23, no. 3, pp. 1097–1104, Mar. 2014.

[13] T. Brox, A. Bruhn, N. Papenberg, and J. Weickert, "High accuracy optical fl w estimation based on a theory for warping," in Proc. 8th ECCV, May 2004, pp. 25–36.

[14] A. Bruhn, J. Weickert, and C. Schnörr, "Lucas/Kanade meets Horn/Schunck: Combining local and global optic fl w methods," Int. J. Comput. Vis., vol. 61, no. 3, pp. 211–231, Feb. 2005.

[15] C. Liu, "Beyond pixels: Exploring new representations and applications for motion analysis," Ph.D. dissertation, Dept. Elect. Eng. Comput. Sci., Massachusetts Inst. Technol., Cambridge, MA, USA, May 2009.

[16] L. Xu, J. Jia, and Y. Matsushita, "Motion detail preserving optical flow estimation," IEEE Trans. Pattern Anal. Mach. Intell., vol. 34, no. 9, pp. 1744–1757, Sep. 2012.

[17] Y. Boykov, O. Veksler, and R. Zabih, "Fast approximate energy min- imization via graph cuts," IEEE Trans.Pattern Anal. Mach.Intell., vol. 23, no. 11, pp. 1222–1239, Nov. 2001.

[18] V. Kolmogorov and R. Zabin, "What energy functions can be minimized via graph cuts?" IEEE Trans. Pattern Anal. Mach. Intell., vol. 26, no. 2, pp. 147–159, Feb. 2004.

[19] J.-L. Starck, M. Elad, and D. L. Donoho, "Image decomposi- tion via the combination of sparse representations and a variational approach," IEEE Trans. Image Process., vol. 14, no. 10, pp. 1570–1582, Oct. 2005.

[20] M. J. Fadili, J.-L.Starck, J. Bobin, and Y. Moudden, "Image decompo- sition and separation using sparse representations: An overview," Proc. IEEE, vol. 98, no. 6, pp. 983–994, Jun. 2010.

[21] M. Elad, Sparse and Redundant Representations: From Theory to Applications in Signal and Image Processing. New York, NY, USA: Springer-Verlag, 2010.

[22] J. Mairal, F. Bach, J. Ponce, and G. Sapiro, "Online learning for matrix factorization and sparse coding," J. Mach. Learn. Res., vol. 11, pp. 19–60, Mar. 2010.

[23] S. G. Mallat and Z. Zhang, "Matching pursuits with time-frequency dictionaries," IEEE Trans. Signal Process., vol. 41, no. 12, pp. 3397–3415, Dec. 1993.

[24] H. Takeda, S. Farsiu, and P. Milanfar, "Kernel regression for image processing and reconstruction," IEEE Trans. Image Process., vol. 16, no. 2, pp. 349–366, Feb. 2007.

[25] C.-C. Chang and C.-J. Lin, "LIBSVM: A library for support vector machines," ACM Trans. Intell. Syst. Technol., vol. 2, no. 3, Apr. 2011, Art. ID 27.